paper. The dependence of the precession frequency on the angle β of deflection of the nuclear magnetization in them is described by the formula $\omega = \omega_0 - \varDelta \cos\beta$. Here, ω_0 is the NMR frequency in the limit of high temperatures, and $\varDelta$ is the dynamic frequency shift. Correspondingly, the energy of the hyperfine interaction varies as $F \sim -\varDelta \sin\beta$, i.e., is a concave function. Consequently, under appropriate conditions BEC of magnons can occur in these magnets. In our experiments of the 1970s, a strange echo signal was observed, whose frequency corresponded to the exciting pulse frequency lying between ω_0 and $\omega_0 - \varDelta$, rather than to the frequency $\omega_0 - \varDelta$ of the linear NMR. We called this effect the capture echo. The capture echo is likely to have been the first observation of the magnon BEC, but this requires additional verification. At present, we are studying the Bose–Einstein condensation of magnons in solid magnets with the support of the Ministry of Education and Science of the Russian Federation (Federal Target Program 'Scientific and Pedagogical Personnel of Innovative Russia', project No. 02.740.11.5217).

Acknowledgments. In conclusion, I wish to emphasize that all our achievements are due to the support of the scientific school of the Institute for Physical Problems, RAS and to that atmosphere of confidence and benevolence which was so ably created by Andrei Stanislavovich Borovik-Romanov.

References

1. Bun'kov Yu M, Dumesh B S, Kurkin M I *Pis'ma Zh. Eksp. Teor. Fiz.* **19** 216 (1974) [*JETP Lett.* **19** 132 (1974)]
2. Bun'kov Yu M, Dumesh B S *Zh. Eksp. Teor. Fiz.* **68** 1161 (1975) [*Sov. Phys. JETP* **41** 576 (1975)]
3. Borovik-Romanov A S, Bunkov Yu M, Dumesh B S *Physica B+C* **86** 1301 (1977)
4. Bun'kov Yu M *Pis'ma Zh. Eksp. Teor. Fiz.* **23** 271 (1976) [*JETP Lett.* **23** 244 (1976)]
5. Bun'kov Yu M, Gladkov S O *Zh. Eksp. Teor. Fiz.* **71** 2181 (1977) [*Sov. Phys. JETP* **46** 1141 (1977)]
6. Bun'kov Yu M, Maksimchuk T V *Zh. Eksp. Teor. Fiz.* **79** 1408 (1980) [*Sov. Phys. JETP* **52** 711 (1980)]
7. Borovik-Romanov A S et al. *Usp. Fiz. Nauk* **142** 537 (1984) [*Sov. Phys. Usp.* **27** 235 (1984)]
8. Lee D M, Richardson R C, in *The Physics of Liquid and Solid Helium* Vol. 2 (Eds K H Bennemann, J B Ketterson) (New York: Wiley, 1978)
9. Borovik-Romanov A S, Bun'kov Yu M, Dmitriev V V, Mukharskii Yu M *Pis'ma Zh. Eksp. Teor. Fiz.* **39** 390 (1984) [*JETP Lett.* **39** 469 (1984)]
10. Fomin I A *Pis'ma Zh. Eksp. Teor. Fiz.* **39** 387 (1984) [*JETP Lett.* **39** 466 (1984)]
11. Borovik-Romanov A S, Bun'kov Yu M, Dmitriev V V, Mukharskii Yu M *Pis'ma Zh. Eksp. Teor. Fiz.* **40** 256 (1984) [*JETP Lett.* **40** 1033 (1984)]
12. Fomin I A *Pis'ma Zh. Eksp. Teor. Fiz.* **40** 260 (1984) [*JETP Lett.* **40** 1037 (1984)]
13. Bunkov Yu M, in *Low Temperature Physics* (Ed. A S Borovik-Romanov) (Moscow: MIR Publ., 1985) p. 132
14. Bunkov Yu M *Prog. Low Temp. Phys.* **14** 69 (1995)
15. Giannetta R W, Smith E N, Lee D M *J. Low Temp. Phys.* **45** 295 (1981)
16. Corruccini L R, Osheroff D D *Phys. Rev. B* **17** 126 (1978)
17. Masuhara N et al. *Phys. Rev. Lett.* **53** 1168 (1984)
18. Borovik-Romanov A S et al. *Zh. Eksp. Teor. Fiz.* **88** 2025 (1985) [*Sov. Phys. JETP* **61** 1199 (1985)]
19. Borovik-Romanov A S et al. *Pis'ma Zh. Eksp. Teor. Fiz.* **45** 98 (1987) [*JETP Lett.* **45** 124 (1987)]
20. Borovik-Romanov A S et al. *Phys. Rev. Lett.* **62** 1631 (1989)
21. Borovik-Romanov A S et al. *Pis'ma Zh. Eksp. Teor. Fiz.* **47** 400 (1988) [*JETP Lett.* **47** 478 (1988)]
22. Borovik-Romanov A S et al. *J. Physique* **49** (C-8) 2067 (1988)
23. Bun'kov Yu M, Dmitriev V V, Mukharskii Yu M *Pis'ma Zh. Eksp. Teor. Fiz.* **43** 131 (1986) [*JETP Lett.* **43** 168 (1986)]
24. Bunkov Yu M, Dmitriev V V, Mukharskiy Yu M *Physica B* **178** 196 (1992)
25. Borovik-Romanov A S et al. *Physica B* **165** 649 (1990)
26. Bunkov Yu M et al. *Europhys. Lett.* **8** 645 (1989)
27. Bunkov Yu M, Lvov V S, Volovik G E *Pis'ma Zh. Eksp. Teor. Fiz.* **83** 624 (2006) [*JETP Lett.* **83** 530 (2006)]
28. Bunkov Yu M, Lvov V S, Volovik G E *Pis'ma Zh. Eksp. Teor. Fiz.* **84** 349 (2006) [*JETP Lett.* **84** 289 (2006)]
29. Bunkov Y M, Golo V L *J. Low Temp. Phys.* **137** 625 (2004)
30. Surovtsev E V, Fomin I A *Pis'ma Zh. Eksp. Teor. Fiz.* **90** 232 (2009) [*JETP Lett.* **90** 211 (2009)]
31. Bunkov Yu M et al. *Phys. Rev. Lett.* **68** 600 (1992)
32. Bunkov Yu M et al. *Physica B* **194–196** 827 (1994)
33. Bunkov Yu M, Volovik G E *Phys. Rev. Lett.* **98** 265302 (2007)
34. Coleman S *Nucl. Phys. B* **262** 263 (1985)
35. Bunkov Yu M et al., arXiv:1002.1674
36. Bunkov Yu M, Volovik G E *Europhys. Lett.* **21** 837 (1993)
37. Kunimatsu T et al. *Pis'ma Zh. Eksp. Teor. Fiz.* **86** 244 (2007) [*JETP Lett.* **86** 216 (2007)]
38. Sato T et al. *Phys. Rev. Lett.* **101** 055301 (2008)
39. Bunkov Yu M, Volovik G E *Pis'ma Zh. Eksp. Teor. Fiz.* **89** 356 (2009) [*JETP Lett.* **89** 306 (2009)]
40. Hunger P, Bunkov Y M, Collin E, Godfrin H *J. Low Temp. Phys.* **158** 129 (2010)
41. Bun'kov Yu M, Volovik G E *Zh. Eksp. Teor. Fiz.* **103** 1619 (1993) [*JETP* **76** 794 (1993)]
42. Dmitriev V V et al. *Phys. Rev. B* **59** 165 (1999)
43. Malomed B A et al. *Phys. Rev. B* **81** 024418 (2010)
44. Volovik G E *J. Low Temp. Phys.* **153** 266 (2008)
45. Bunkov Yu M, Volovik G E *J. Phys. Condens. Matter* **22** 164210 (2010)
46. Bunkov Yu M, Volovik G E, arXiv:1003.4889

PACS numbers: 03.75.Hh, 75.30.Ds, **75.45.+j**
DOI: 10.3367/UFNe.0180.201008n.0890

Kinetics and Bose–Einstein condensation of parametrically driven magnons at room temperature

O Dzyapko, V E Demidov, S O Demokritov

The origin of the ferromagnetic state is the quantum-mechanical exchange interaction between spins of individual atoms, which aligns the spins in parallel to each other. The paramagnet–ferromagnet transition is documented by a divergence of the coherence length describing the correlation between the longitudinal components of the spins located far from each other. The fluctuations above the ground state of a ferromagnet with totally parallel spins are usually described by means of quantized low-energy spin-wave excitations, which are called magnons. Magnons in thermal equilibrium do not show coherence effects because at nonzero temperatures the transverse spin components remain uncorrelated even in a ferromagnetic phase. In fact, they are usually considered to form a gas of elementary excitations (quasi-

O Dzyapko, V E Demidov, S O Demokritov Institut für Angewandte Physik, Westfälische Wilhelms-Universität Münster, Deutschland
E-mail: demokrit@wwu.de

Uspekhi Fizicheskikh Nauk **180** (8) 890 – 894 (2010)
DOI: 10.3367/UFNr.0180.201008n.0890
Translated by S O Demokritov; edited by A Radzig

particles), nicely described by the quantum representation of population numbers. There have been attempts to describe coherent magnon states [1] by analogy to coherent photon states [2]. However, this description has not been well developed and has not been widely used yet for the analysis of experimental results.

Magnons are Bose particles; therefore, under particular conditions they should demonstrate Bose-Einstein condensation (BEC). However, to reach BEC at room temperature one needs to increase the chemical potential of the magnon gas above the zero value characterizing the state of true thermal equilibrium. Here we present our recent results on BEC in magnon gas driven by microwave pumping. The room-temperature kinetics and thermodynamics of magnon gas was investigated by means of the Brillouin light scattering (BLS) technique. We show that for high enough pumping powers the relaxation of the driven gas results in a quasiequilibrium state described by the Bose–Einstein statistics with a nonzero chemical potential. A further increase in the pumping power causes BEC in the magnon gas, documented by an observation of the magnon accumulation at the lowest energy level. Interference of two magnon condensates is observed as well.

One of the most striking quantum phenomena leading to spontaneous quantum coherence on a macroscopic scale is Bose–Einstein condensation. It describes the formation of a collective quantum state of bosons. As the temperature T of the boson gas decreases at a given density N or, vice versa, the number of particles increases at a given temperature, the chemical potential μ describing the gas increases as well. On the other hand, μ cannot be larger than the minimum energy of the bosons, $\varepsilon_{\min}$. The condition $\mu(N, T) = \varepsilon_{\min}$ defines a critical density $N_c(T)$. If the density of the particles in the system is larger than N_c, BEC takes place: the gas is spontaneously divided into two fractions, namely (i) incoherent particles with the density N_c distributed over the entire spectrum of possible boson states, and (ii) a coherent ensemble of particles accumulated in the lowest state with $\varepsilon = \varepsilon_{\min}$ [3].

At temperatures far below the temperature T_c of magnetic ordering, magnons can be considered as weakly interacting bosons: the Bloch law for the temperature dependence of static magnetization, which nicely describes a bulk amount of experimental data, has been obtained based on this assumption. Since magnons are bosons one can expect that they undergo the BEC transition. Several groups have reported observation of the magnetic field-induced BEC of magnetic excitations in the quantum antiferromagnets $TlCuCl_3$ [4, 5], Cs_2CuCl_4 [6, 7], and $BaCuSi_2O_6$ [8]. In these materials, a phase transition from a nonmagnetic singlet state to an ordered triplet state, accompanied by magnetic mode softening, occurs if the applied magnetic field is strong enough to overcome the antiferromagnetic exchange coupling. Such a transition can be treated as BEC in an ensemble of magnetic excitations. However, these excitations can hardly be considered as magnons — quanta of spin precession waves propagating in a magnetically ordered system.

BEC has also been observed in the ensemble of nuclear spins in superfluid ^{3}He at temperatures in the millikelvin range [9, 10]. A cell with superfluid ^{3}He was put in a strong gradient of a magnetic field. The spins were pumped by the radio-frequency radiation at the frequencies of nuclear magnetic resonance (NMR). In a pulsed NMR experiment, the magnetization of the nuclear spins was deflected by a strong pulse of the radio-frequency field, and an induction signal of the total magnetization of ^{3}He in the cell was detected by pick-up coils after the pumping pulse was switched off. Upon terminating the external pumping, the total induction signal dephased and disappeared in about 1 ms due to the strong gradient of magnetic field over the cell. However, after a transient process of about 10 ms, the induction signal corresponding to a 100% coherent precession of the deflected magnetization was detected over a long period of time up to 0.3–0.5 s. This effect is a direct manifestation of the BEC of magnons in ^{3}He.

Very recently it was shown that magnons continuously driven by microwave parametric pumping can enormously overpopulate the lowest energy level, even at room temperature [11]. This observation has been associated with the BEC of magnons. At the same time, the possibility of the BEC of quasiparticles in the thermodynamic sense is not evident [12], since quasiparticles are characterized by a finite lifetime which is often comparable to the time a system needs to reach thermal equilibrium. Moreover, an observation of the spontaneous coherence is important proof of the existence of BEC [13]. Therefore, the study of the thermalization processes for a gas of magnons and the experimental observation of the spontaneous coherence of the magnons overpopulating the lowest state are of special importance for a clear understanding of the phase transition observed in the earlier work [11].

The transition temperature of BEC in a weakly interacting gas of Bose particles with a given total density N of the particles is determined by the Einstein equation $k_B T_c = 3.31(\hbar^2/m)\, N^{2/3}$. This equation does not imply that the transition temperature should be low. Moreover, the above equation can be rewritten as $N_c^{2/3} = k_B T m/(3.31\hbar^2)$. In other words, the BEC transition can be reached at any temperature, provided the density of the particles is high enough. Below, we will demonstrate how the BEC transition can be observed at room temperature.

Experiments on the room-temperature BEC of magnons were performed on monocrystalline films of yttrium iron garnet (YIG) with a thickness of 5 μm. YIG ($Y_3Fe_2(FeO_4)_3$) is one of the most studied magnetic substances. YIG films are characterized by very small magnetic losses providing a long magnon lifetime in this substance: it appears to be much longer than the characteristic time of magnon–magnon interaction [13, 14]. This relation is a necessary precondition for Bose–Einstein condensation in a gas of quasiparticles whose number is not exactly conserved [12]. Samples with lateral sizes of several millimeters were cut from the films and were placed into a static uniform magnetic field of $H = 700-1000$ Oe oriented in the plane of the film. The injection of the magnons was performed by means of parallel parametric pumping with a frequency of 8.0–8.1 GHz. The pumping field was created using a microstrip resonator with a width of 25 μm attached to the surface of the sample. The peak pumping power was varied from 0.1 to 6 W. Details on the pumping process can be found in Refs [11, 13–15].

The redistribution of magnons over the spectrum was studied with a temporal resolution of 10 ns using time-resolved BLS spectroscopy in the quasibackward scattering geometry [16]. In this geometry, magnons from the wave vector interval $k = \pm 2 \times 10^5$ cm^{-1} determined by the wave vector of the incident light contribute to BLS spectra. Thus, the BLS intensity at a given frequency is the product of the magnon population at this frequency and the reduced density of magnon states, taking into account the above wave vector interval alone. Giving access to the measurement of the temporal evolution of the magnon distribution, the BLS technique allows one to study the kinetics and thermodynamics of magnons. A typical frequency resolution of the experimental setup, limited by the resolution of the optical spectrometer, was 250 MHz. It was also possible to achieve a better resolution of $\Delta f = 50$ MHz, albeit at the expense of sensitivity [11]. The experiments were performed at room temperature. A detailed description of the BLS setup used can be found elsewhere [11, 13–16]

Figure 1 shows the low-frequency part of the dispersion spectrum of magnons in an in-plane magnetized ferromagnetic film, calculated for the parameters of the YIG film used and a magnetic field of $H = 700$ Oe. The solid lines represent the dispersion curves for the two limiting cases of magnons with the wave vectors **k** oriented parallel (so-called backward volume waves) or perpendicularly (so-called surface waves) to the static magnetic field **H** as indicated in Fig. 1. The both curves merge for $k = 0$ at the frequency of the uniform ferromagnetic resonance. The magnon states for intermediate angles fill the manifold between these two boundaries. As seen from Fig. 1, the manifold is characterized by a nonzero minimum frequency $f_{\rm min} = 2.10$ GHz corresponding to a nonzero wave vector $k_{\rm min} = 3 \times 10^4$ cm^{-1} aligned in parallel to the static magnetic field. The frequency minimum at a nonzero wave vector results from competition between the magnetic dipole interaction and the exchange interaction. Note that the change in the external magnetic field shifts $f_{\rm min}$, whereas by varying the film thickness one varies the corresponding wave vector $k_{\rm min}$.

Figure 1 also illustrates the process of the parametric pumping of the magnon gas. This process can be considered as the creation of two primary magnons by a microwave photon of the pumping field. It does not define the values of the magnon wave vectors. The only condition is that the two created magnons have opposite wave vectors. The pumping initiates a strongly nonequilibrium magnon distribution: a very high density of primary magnons amounting to $10^{18} - 10^{19}$ cm^{-3} is created in the phase space close to the frequency $f_{\rm p}$. Although the primary magnons are excited by coherent pumping, they are not coherent to each other: two magnons are excited simultaneously, and only the sum of their phases, but not the phase of each magnon, is locked to the phase of the microwave pumping photon.

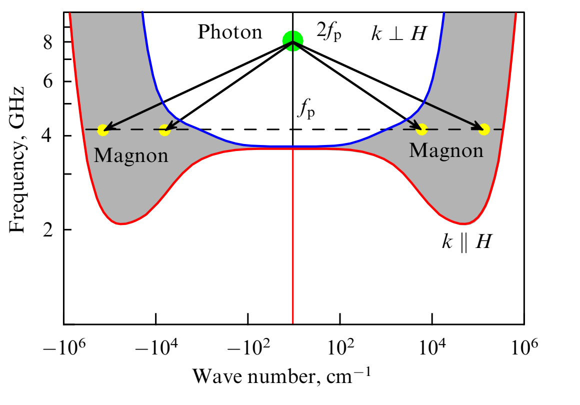

Figure 1. The low-frequency part of the dispersion spectrum of magnons in a YIG film magnetized by an in-plane static magnetic field $H = 700$ Oe. The arrows illustrate the process of parametric pumping.

Due to the intense magnon–magnon interaction, the primary magnons are rapidly redistributed over the phase space. The main mechanisms responsible for the energy redistribution *within* the magnon system are the two-magnon and the four-magnon scattering processes (see chapter 11 in book [14]). Four-magnon scattering dominates in high-quality epitaxial YIG films. It can be considered as an inelastic scattering mechanism, since it changes the energies of the scattered magnons. As a consequence, four-magnon scattering leads to the spreading of the magnons over the spectrum, keeping, however, the number of magnons in the system constant. Note here that the three-magnon scattering process which does not conserve the number of magnons does not play an important role in the described experiments [15]. In parallel, an energy transfer *out* of the magnon system due to the spin–lattice (magnon–phonon) interaction takes place. It will be shown below that the magnon–magnon scattering mechanisms preserving the number of magnons are much faster than spin–lattice relaxation. Under these conditions, a stepwise pumping should create a magnon gas characterized by a steady, quasiequilibrium distribution of magnons over the phase space after a certain transition period characterized by a thermalization time.

The magnon distributions illustrating the evolution of the magnon gas to the quasiequilibrium state are plotted in Fig. 2 for a pumping power of 0.7 W. This figure presents BLS spectra recorded for different delay times after the start of the pumping pulse. At the delay time $t = 0$, no magnons are pumped yet, and the magnon distribution corresponds to thermally excited magnons. In the early pumping stage ($t = 30$ ns), the population of magnon states close to $f_{\rm min}$ is not affected at all. On the contrary, the magnon density at frequencies from about 2.5 GHz to 4 GHz (the latter is close to the frequency of the primary magnons) rises significantly. Further evolution of the magnon distribution presented in Fig. 2 shows a saturation of the magnon population. In fact, the magnon population of the entire spectrum except the region close to $f_{\rm min}$ is saturated at $t = 60$ ns. The density of magnons close to $f_{\rm min}$ starts to grow for $t > 30$ ns and saturates for much larger delays, as shown in Fig. 3. The observed process can be understood as a gradual wavelike population of magnon states starting from the frequency $f_{\rm p}$ of primary magnons towards the minimum magnon frequency.

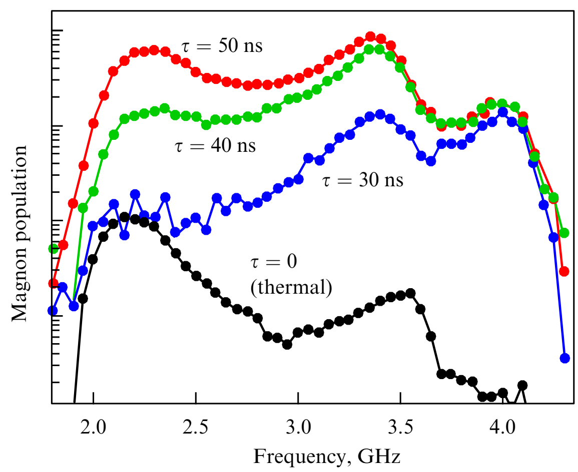

Figure 2. Evolution of the magnon population after stepwise pumping has been switched on. Note the wavelike increase in the magnon population propagating from higher frequencies toward the bottom of the spectrum.

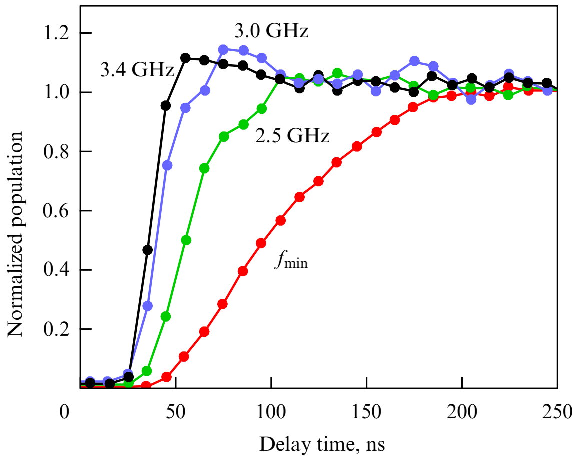

Figure 3. Evolution of the magnon population at different frequencies as a function of the delay time after stepwise pumping has been switched on. Note the slow (adiabatic) increase in the population at $f_{\min}$.

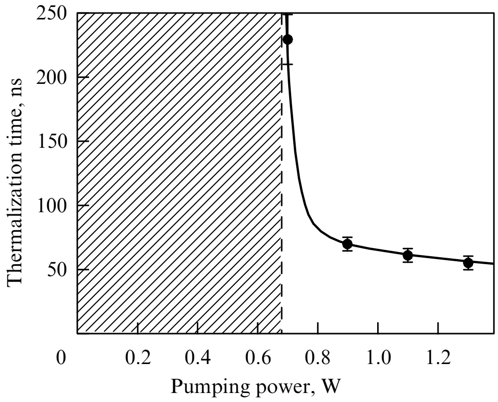

Figure 4. The magnon gas thermalization time as a function of the pumping power. The shaded area corresponds to the power below the thermalization threshold $P_{\text{th}} = 0.7$ W, where the thermalization cannot be achieved. The solid line is a guide for the eye.

This means that the increase in the population at the bottom of the spectrum takes place through multiple inelastic scattering events. Thus, a very important intermediate conclusion can be made at this point: since the magnons close to $f_{\min}$ are created through a series of multiple scattering events not conserving the phase of individual magnons, any coherence observed in the gas of magnons at the bottom of the spectrum must be a spontaneous one.

After the magnon population at the bottom of the spectrum saturates, the entire magnon gas reaches a steady state. Comparison of the measured distribution with the Bose–Einstein one confirms that this steady state corresponds to a quasiequilibrium thermodynamic state.

Due to the nonlinearity of the four-magnon scattering, the magnon thermalization time also rapidly decreases with increasing pumping power above the threshold of 0.7 W, as illustrated by Fig. 4. As seen in the figure, the thermalization time approaches a value of about 50 ns at the pumping power of 1.3 W, which is significantly lower than the lifetime of magnons in YIG films due to the spin–lattice interaction. The shaded area in the figure indicates the region of lower pumping powers, where complete thermalization of a magnon gas cannot be achieved.

After the thermal quasiequilibrium is reached, further pumping increases the density of magnons as a function of time. As a result, the value of the chemical potential μ increases as well. For the values of the pumping powers used in the experiments, this growth in μ happens much more slowly than the thermalization process; therefore, it can be considered adiabatic. Figures 5a and 5b show the measured BLS spectra at large delay times, reflecting the quasiequilibrium distributions of magnons over the phase space at different pumping powers $P = 4$ W and 5.9 W, respectively. Tokens in the figures represent the experimental data, and solid lines are the magnon distributions calculated based on the Bose–Einstein statistics [15], using μ as the fit parameter. As seen in Fig. 5a, the chemical potential grows with time, reaching saturation at $\mu/h = 2.08$ GHz. This value is close to but still below $\varepsilon_{\min} = hf_{\min}$. Apparently, higher values of μ

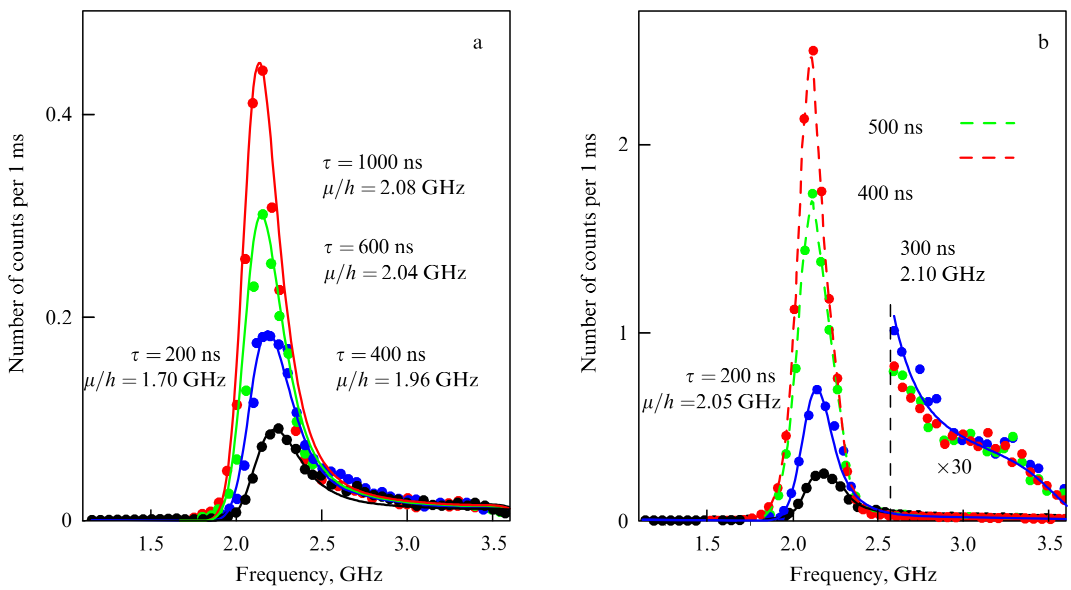

Figure 5. (a) BLS spectra from pumped magnons at a pumping power of 4 W at different delay times, as indicated. Solid lines show the results of the fit of the spectra based on the Bose–Einstein statistics, with the chemical potential being a fit parameter. Note that the critical value of the chemical potential cannot be reached at the power used. (b) Same as figure (a) for the pumping power 5.9 W. The critical value of the chemical potential is reached at 300 ns.

cannot be reached at this pumping power, since the pumped magnons leave the magnon gas due to spin–lattice relaxation. Figure 5b illustrates the processes at $P = 5.9$ W. For this pumping power, the maximum value of $\mu/h = 2.10$ GHz is reached already after 300 ns. One can conclude that the critical density N_c of the magnon gas is achieved at $t = 300$ ns, and the corresponding distribution can be considered as the critical distribution $n_c(f)$. Further pumping leads to a phenomenon which can indeed be interpreted as the BEC of magnons: all additionally pumped magnons are collected at the bottom of the spectrum without changing the population of the states with higher frequencies. This last fact is demonstrated in Fig. 5b as well, showing the high-frequency parts of the magnon distribution curves on an appropriate scale. These data demonstrate that the BLS spectra for $t > 300$ ns cannot be described just by increasing the temperature in the Bose–Einstein distribution function, since a higher temperature means higher magnon populations at *all* frequencies. Thus, Fig. 5b testifies to a formation of a Bose–Einstein condensate of magnons.

One can calculate the difference between the magnon distribution at a given time $t > 300$ ns and the critical one. One can see from Fig. 5b that this difference is nonzero just in the region close to $f_{\min}$, with the width of the region $\Delta f \approx 0.2-0.3$ GHz being defined by the resolution of the spectrometer. Optical measurements with ultimate spectral resolution have shown that the intrinsic width of the region is even below 50 MHz. Moreover, microwave spectroscopy indicates that it is narrower than 4 MHz, which corresponds to a high degree of coherence of magnons in the condensate, giving $\Delta f < 10^{-6} k_B T/h$. Thus, the narrowing of the magnon distribution with respect to that determined by the classical Boltzmann statistics is more than six orders of magnitude!

The ultimate confirmation of coherence of the observed collective quantum state might be interference of two condensates with each other. In the system studied, such an experiment can be performed in a direct way. Indeed, the magnon spectrum exhibits two degenerate minima at $k_{\min} = \pm 3 \times 10^4$ cm^{-1}; therefore, two condensates with different wave vectors are created simultaneously. The interference between them should result in a standing wave of the condensate density in real space. Figure 6a illustrates the measured profile of the condensate density. It is worth noting that, contrary to previous experiments, these measurements were not performed stroboscopically. Since each pumping pulse creates a condensate with an arbitrary phase, the phase difference between the two condensates should vary from event to event. Therefore, to detect the interference between two condensates, the pumping was applied continuously. For this purpose, a resonator allowing continuous pumping without significant overheating was designed. Thus, the values of the applied pumping powers, which allow the condensation, do not match the pumping powers corresponding to the data given in Fig. 5.

The presented profiles clearly indicate a standing wave, resulting from the interference of two condensates. To emphasize the formation of the standing wave, the Fourier transforms of the shown profiles were calculated, as illustrated in Fig. 6b. As seen from the figure, the Fourier spectra at higher pumping powers exhibit a peak whose position nicely coincides with the double value of the wave vector $k_{\min} = \pm 3 \times 10^4$ cm^{-1}. Thus, Fig. 6 undoubtedly demonstrates the coherence of the created condensates.

In conclusion, we have investigated the thermalization of a magnon gas driven by microwave parametric pumping to a quasiequilibrium state with a nonzero chemical potential. For a certain critical value of the pumping power, Bose–Einstein condensation of magnons occurs. The results obtained are in accordance with the concept of Bose–Einstein condensation and give undoubted experimental evidence of the existence of a Bose–Einstein condensate at room temperature.

Support from the Deutsche Forschungsgemeinschaft is gratefully acknowledged. S.O.D. would like to emphasize the important role of A S Borovik-Romanov in his scientific carrier.

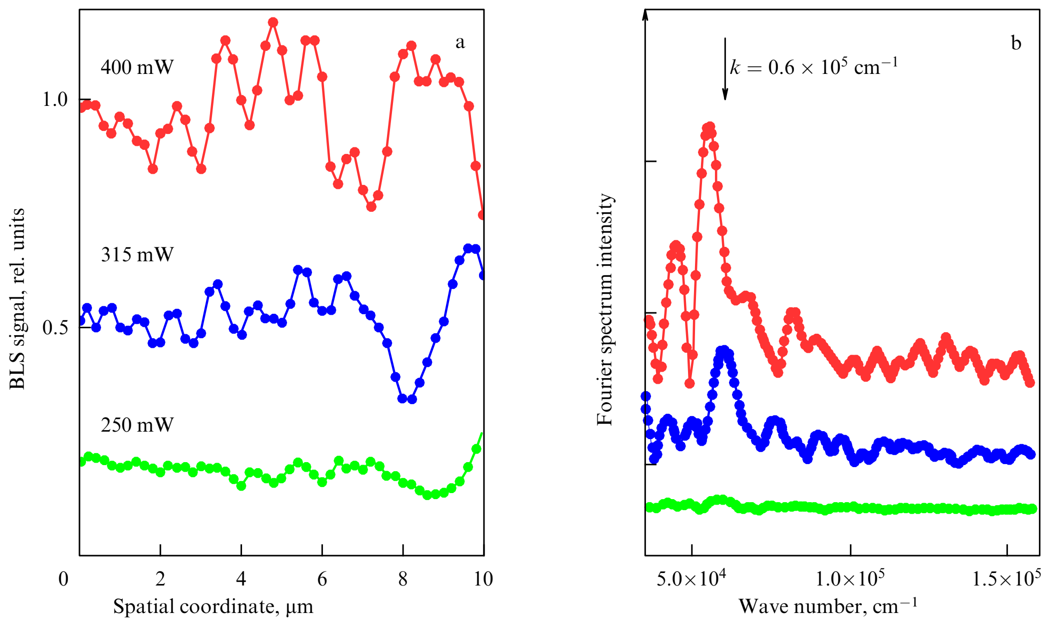

Figure 6. (a) BLS signal from two interfering condensates measured with a spatial resolution of 250 nm; (b) Fourier spectra of the spatial profiles presented in figure (a). The arrow indicates the position of the maximum calculated based on the magnon dispersion.

References

1. Rezende S M, Zagury N *Phys. Lett. A* **29** 47 (1969)
2. Glauber R J *Phys. Rev.* **131** 2766 (1963)
3. Einstein A "Quantentheorie des einatomigen idealen Gases" *Sitzungsberichte Preuß. Akad. Wiss. Berlin* **1** 3 (1925)
4. Nikuni T et al. *Phys. Rev. Lett.* **84** 5868 (2000)
5. Rüegg Ch et at. *Nature* **423** 62 (2003)
6. Coldea R et al. *Phys. Rev. Lett.* **88** 137203 (2002)
7. Radu T et al. *Phys. Rev. Lett.* **95** 127202 (2005)
8. Jaime M et al. *Phys. Rev. Lett.* **93** 087203 (2004)
9. Bunkov Yu M, Volovik G E *J. Low Temp. Phys.* **150** 135 (2008)
10. Volovik G E *J. Low Temp. Phys.* **153** 266 (2008)
11. Demokritov S O et al. *Nature* **443** 430 (2006)
12. Snoke D *Nature* **443** 403 (2006)
13. Demidov V E et al. *Phys. Rev. Lett.* **100** 8047205 (2008)
14. Demidov V E et al. *Phys. Rev. Lett.* **99** 037205 (2007)
15. Dzyapko O et al. *New J. Phys.* **9** 64 (2007)
16. Demokritov S O, Hillebrands B, Slavin A N *Phys. Rep.* **348** 441 (2001)
17. Sparks M *Ferromagnetic-Relaxation Theory* (New York: McGraw-Hill, 1964)